Global Λ Polarization in high energy collisions

Yilong Xie[1], Dujuan Wang[2], and László P. Csernai[1]
[1] *Institute of Physics and Technology, University of Bergen, Allegaten 55, 5007 Bergen, Norway*
[2] *School of Science, Wuhan University of Technology, 430070, Wuhan, China*
(Dated: March 16, 2017 - v6)

With a Yang-Mills flux-tube initial state and a high resolution (3+1)D Particle-in-Cell Relativistic (PICR) hydrodynamics simulation, we calculate the Λ polarization for different energies. The origination of polarization in high energy collisions is discussed, and we find linear impact parameter dependence of the global Λ polarization. Furthermore, the global Λ polarization in our model decreases very fast in the low energy domain, and the decline curve fits well the recent results of Beam Energy Scan (BES) program launched by the STAR collaboration at the Relativistic Heavy Ion Collider (RHIC). The time evolution of polarization is also discussed.

PACS numbers: 25.75.-q, 24.70.+s, 47.32.Ef

arXiv:1703.03770v2 [nucl-th] 14 Mar 2017

I. INTRODUCTION

The nontrivial polarization effect in high energy collisions, since it was firstly observed in Fermilab with both polarized and unpolarized incident beam [1, 2], had been raising people's interest. The Λ hyperon is well suited to measure the polarization because through the decay $\Lambda^0 \rightarrow p + \pi^-$ with proton carrying the spin information, the Λ becomes its own spin-analyzer. Afterwards, more experimental research had been launched continuously, including nucleon collisions and heavy ion collisions [3–9]. Theoretical studies have also been underway synchronously with the experiments [10–19].

These experiments had observed that, 1) the Λ polarization is perpendicular to the reaction plane, 2) and increases with the Λ's transverse momentum (p_T) and its Feynman-x, taken to be $x_F = p_L/\sqrt{s}$ [4, 5, 7]. However, no significant evidence was found to indicate the energy dependence of the hyperon polarization, which we will discuss in this paper.

The Λ polarization in experiments was measured through the angular distribution of emitted protons in Λ's rest frame:

$$\frac{dN}{dcos\theta} = (1 + \alpha P cos\theta)/4\pi, \tag{1}$$

where θ is the angle between the proton momenta $\boldsymbol{p}_p$ and the Λ's spin $\boldsymbol{S}_\Lambda$, P is the polarization amplitude, and the decay parameter α is taken to be 0.647 ± 0.013 [1, 8]. To perform the measurement and calculation, it is crucial to determine the Reaction Plane (RP) and Center of Mass (CM) of the participant system. Recently it was pointed out that in collider experiments the CM frame determination might not be accurate enough due to the nuclear fragmentation effects while the early fixed target experiments can get rid of this issue [20].

From the experiments, theorist suggested that the hyperon polarization originates from the initial substantial angular momentum, $\boldsymbol{L}$, in non central collisions, since the global polarization aligns with the orbital angular momentum. The initial angular momentum is dependent on impact parameter, or centrality percentage, taking a shape of quadratic function that peaks around 9% centrality percentage, as shown in Refs. [21, 22]. In the RHIC's Au+Au collisions at 62.4 GeV and 200 GeV, no centrality dependence of the global hyperon polarization was analyzed [23], due to the insignificant polarization. Recently, stronger polarization signal was observed in RHIC's Beam Energy Scan (BES) program in the energy region below 100 GeV [24]. Therefore, in this paper we will try to explore this issue again.

During the past decades, two different perspectives were developed for the transition mechanism from initial angular momentum to the final state hyperon polarization, i.e. the hydrodynamical perspective and partonic kinetic perspective. From the partonic microperspective, the initial angular momentum is transferred to the partons through the interaction of spin-orbit coupling in viscous QGP [11], and then the global polarized quarks are recombined into hadrons, in which the Thomas precession of the quark spin was applied [25].

In the hydro- and thermo- dynamical description, the initial angular momentum is manifested in a longitudinal velocity shear, which, with small shear viscosity, results into a rotating system with substantial vorticity and even Kelvin-Helmholtz instability [26]. Assuming local equilibrium at freeze out and equipartition of the spin degree of freedom, Ref. [15] put forward a polarization 3-vector for spin 1/2 particles and antiparticles based on the generalization of Cooper-Frye formula for particles with spin.

It was recently pointed out that the detailed balance of Cooper-Frye formula on Freeze-Out(FO) hypersurface requires a non-vanishing polarization in fluid before FO [27]. However, the absence of pre-FO polarization should not significantly effect the polarization calculation based on Ref. [15]. One can calculate that, the spin of each baryon is $L = \hbar/2 \approx 98.5\, MeV\cdot fm/c$. As the polarization is between 1 - 10 % at different beam energies in the RHIC BES program, this gives $L \approx 1 - 10\, MeV\cdot fm/c$ for the angular momentum carried by one baryon. On the other hand the total angular momentum is around [28]: $L = 1.05 \times 10^4 \hbar = 205.8 \times 10^4\, MeV\cdot fm/c$. This is distributed among a few hundred baryons in semi-peripheral reactions at not too high energies, i.e. very

few antibaryons, which gives an angular momentum per baryon: $L \approx 10^4\, MeV \cdot fm/c$. This is 3 - 4 orders of magnitude bigger than the spin angular momentum carried by one baryon in the vortical flow. Therefore, even if 1 - 10% of spins are already polarized before FO, carrying only one per mil of the total angular momentum, they will neither effectively impact the fluid dynamical evolution, nor significantly change the detailed balance during FO process, thus keeping the validity of the polarization 3-vector in Ref. [15].

Refs. [17, 18] applied this polarization 3-vector to relativistic heavy ion collisions, to explore the momentum space distribution of Λ polarization. However, the previously neglected second term of the polarization formula, which reflects the effect of system expansion, turned out to be not negligible. In this paper, we will compute the complete Λ polarization, including both the first and second term, for the Au + Au collisions in the same energy domain as the RHIC BES program.

II. Λ POLARIZATION IN HYDRODYNAMIC MODEL

The initial state we used here could naturally generate a longitudinal velocity shear [29, 30], which leads to the hyperon polarization after the hydrodynamical evolution, simulated by a high resolution Computational Fluid Dynamic (CFD) calculation using the Relativistic Particle-in-Cell (PICR) method. This initial state assumed a Yang-Mills field string tension between Lorentz contracted streaks after impact, and conserved the angular momentum both locally and globally. Both in the initial state and subsequent CFD simulation, the frequently used 'Bag Model' EoS was applied: $P = c_0^2 e^2 - \frac{4}{3}B$, with constant $c_0^2 = \frac{1}{3}$ and a fixed Bag constant B [29–31]. The energy density takes the form: $e = \alpha T^4 + \beta T^2 + \gamma + B$, where α, β, γ are constants arising from the degeneracy factors for (anti-)quarks and gluons. At Freeze-Out (FO) stage, the major part of FO hypersurface is assumed to be timelike, which entails small changes between the pre-FO and post-FO state, and thus the ideal gas phase space distribution can be applied [18, 32].

The spatial part of polarization 3-vector for (anti-) hyperon with mass m, reads as [17–19]:

$$\begin{aligned}\mathbf{\Pi}(p) = &\frac{\hbar\varepsilon}{8m}\frac{\int \mathrm{d}\Sigma_\lambda p^\lambda\, n_F\ (\nabla\times\boldsymbol{\beta})}{\int \mathrm{d}\Sigma_\lambda p^\lambda\, n_F}\\ &+\frac{\hbar\mathbf{p}}{8m}\times\frac{\int \mathrm{d}\Sigma_\lambda p^\lambda\, n_F\ (\partial_t\boldsymbol{\beta}+\nabla\beta^0)}{\int \mathrm{d}\Sigma_\lambda p^\lambda\, n_F}\ ,\end{aligned} \tag{2}$$

where $\beta^\mu(x) = (\beta^0, \boldsymbol{\beta}) = [1/T(x)]u^\mu(x)$ is the inverse temperature four-vector field, and $n_F(x,p)$ is the Fermi-Jüttner distribution of the Λ, that is $1/(e^{\beta(x)\cdot p - \xi(x)}+1)$, being $\xi(x) = \mu(x)/T(x)$ with μ being the Λ's chemical potential and p its four-momentum. $\mathrm{d}\Sigma_\lambda$ is the freeze out hypersurface element, for t =const. freeze-out, $\mathrm{d}\Sigma_\lambda p^\lambda \rightarrow \mathrm{d}V\varepsilon$, where $\varepsilon = p^0$ being the Λ's energy.

Here the *first term* reflects the classical vorticity effect ($\nabla\times\beta$), and the *second term* arises from the expansion effect ($\partial_t\boldsymbol{\beta}$) and relativistic modification ($\nabla\beta^0$). Noticing that the convention of $\Pi(p)$ is normalized to 50%, i.e. Eq. (1), the value should be multiplied by 2 to keep in line with the polarization anisotropy in experimental studies, where the upper limit is 100%. This is unlike the previous studies [13, 17–19]. Besides, the Eq. (2) is calculated in the Center-of-Mass (CM) frame, and one can Lorentz boost it into Λ's rest frame by the following formula:

$$\mathbf{\Pi}_0(\boldsymbol{p}) = \mathbf{\Pi}(p) - \frac{\boldsymbol{p}}{p^0(p^0+m)}\mathbf{\Pi}(p)\cdot\boldsymbol{p}\ . \tag{3}$$

The three components of the polarization 3-vectors, $2\mathbf{\Pi}(p_x,p_y)$ (or $2\mathbf{\Pi_0}(p_x,p_y)$) have different significance. As we pointed out in our earlier paper [19], the x and y components of polarization, $2\Pi_x$ and $2\Pi_x$, in transverse momentum space $[p_x,p_y]$ are rather trivial and form a symmetric dipole structure, which results in vanishing global polarization along the x and y direction in the participant CM frame. Meanwhile, as expected, the $-y$ directed polarization, aligned with the initial angular momentum, dominates the modulus of polarization 3-vector, $2|\mathbf{\Pi_0}(\boldsymbol{p_x},\boldsymbol{p_y})|$. Fig. 1 shows the dominant y component and the modulus of Λ polarization, in Au-Au collisions at 11.5 GeV. One can see that the top and down figures have similar structure and magnitude, which indicates a trivial influence of the x and y components on the global polarization.

Since the $-y$ directed global Λ polarization in experimental results is averaged polarization over the Λ's momentum space, we evaluated the average of the y component of the polarization $\langle\Pi_{0y}\rangle_p$. We integrated the y component of the obtained polarization, Π_{0y}, over the momentum space as follows:

$$\begin{aligned}\langle\Pi_{0y}\rangle_p &= \frac{\int dp\,dx\,\Pi_{0y}(p,x)\,n_F(x,p)}{\int dp\,dx\,n_F(x,p)}\\ &= \frac{\int dp\,\Pi_{0y}(p)\,n_F(p)}{\int dp\,n_F(p)}\end{aligned} \tag{4}$$

to calculate the global polarization. The word 'global' means averaging over phase space [$\boldsymbol{x}$, $\boldsymbol{p}$]. Besides, we replace the $\langle\Pi_{0y}\rangle_p$ with $-\langle\Pi_{0y}\rangle_p$, since in experiments the angular momentum's direction, i.e. negative y direction is the conventional direction for global polarization.

III. RESULTS AND DISCUSSION

A. Angular momentum, Impact Parameter and Centrality

According to the alignment of polarization and the system's angular momentum, theorists suggested to attribute the polarization to the initial orbital angular momentum arising in non-central collisions. Refs. [21, 22] have analytically deduced and schematically displayed

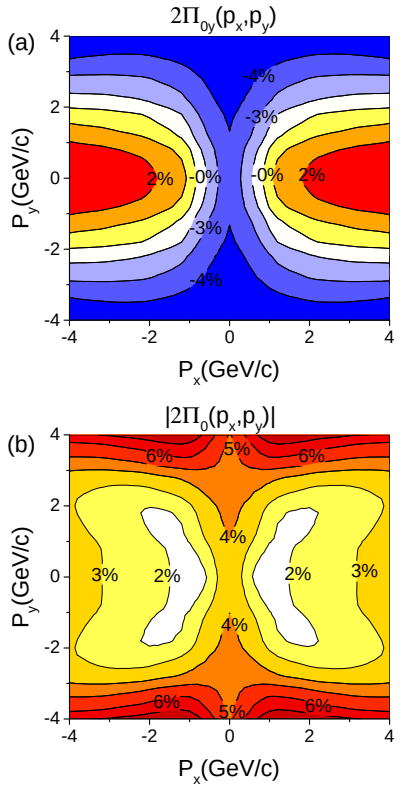

FIG. 1. (Color online) The y component (top) and the modulus (bottom) of the Λ polarization for momentum vectors in the transverse, $[p_x, p_y]$, plane at $p_z = 0$, for the Au+Au reaction at $\sqrt{s_{NN}} = 11.5$ GeV. The figure is in the frame of the Λ. The impact parameter $b = 0.7b_m = 0.7 \times 2R$, where R is the radius of Au and $b_m = 2R$ is the maximum value of b. The freeze out time is $6.25 = (2.5 + 4.75)$ fm/c, including 2.5 fm/c for initial state and 4.75 fm/c for hydro-evolution.

the initial angular momentum in the reaction region as a function of impact parameter b, taking the form of quadratic function, which roughly peaks at $b = 0.25b_m$ or $0.3b_m$. If the angular momentum is translated into polarization without any other significant perturbative mechanism, one should also observe the polarization's dependence on impact parameter. In other words, the initial angular momentum of the participant system is initiated by the inequality of local nuclear density in the transverse plane, and this inequality is dependent on the impact parameter. Thus the initial impact parameter dependence of the late-state polarization should in principle be observed.

Fig. 2 shows the global polarization of Au+Au collisions as a function of ratio of impact parameter b to Au's nuclear radius R, i.e. $b_0 = b/2R$. One could see that the polarization at different energies indeed approximately takes a linear increase with the increase of impact parameter, except for 62.4GeV due to the vanishing polarization signals at relatively central collisions. This linear dependence clearly indicates that the polarization in our model arises from the initial angular momentum. However, the polarization's linear dependence on b is somewhat different from the angular momentum's quadratic dependence on b. This is because the angular momentum L is an extensive quantity dependent on the system's mass, while the polarization Π is an intensive quantity.

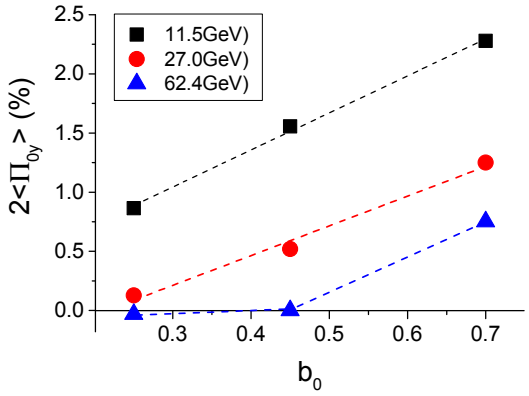

FIG. 2. (Color online) The linear dependence of global polarization, $2\langle\Pi_{0y}\rangle_p$, as a function of impact parameter ratio b_0 at 11.5 GeV, 27.0 Gev and 62.4 GeV.

An earlier Λ global polarization measurement by STAR in Au+Au collisions at 62.4 GeV and 200 GeV, had observed a not significant indication of centrality dependence, due to the occurrence of negative polarization, as well as large error bars [9, 33]. The result of opposite directed global polarization at different centralities would be weird, if we assume that polarization comes from the angular momentum. Besides, no experimental Λ polarization measurements, previous to the present ones had observed the opposite pointing direction of global Λ polarization [1–6]. This might be because of the inappropriate choice of momentum space. However, from the Figs. 5 and 7 in Ref. [9, 33] one could still see that, the polarization signal becomes stronger at larger centrality, while at small centrality percentage (below 40%) the signal is weak and vanishing. Similar behavior occurs in our simulation results for 62.4 GeV, specifically the polarization value also vanishes when the centrality percentage goes below 20%, and increases as the centrality increases.

The recently reported global Λ polarization observation in STAR's BES I program has shown a positive signal for both Λ and $\bar{\Lambda}$, thus it is promising to eliminate the disturbing opposite polarization direction that occurred in previous experiments [1–6], and this confirm our predictions. Besides, the RHIC's Event Plane Detector (EPD) on upgrading for future BES II with higher EP resolution, will provide a better chance to determine the issue of centrality dependence of Λ polarization [34]. With experimental CM identification one could also verify the momentum dependence of the polarization as shown in Fig. 1.

B. Energy Dependence and Time evolution

The Λ polarization increases with its Feynman-$x_F = p_L/\sqrt{s}$, as well as transverse momentum p_T, had been observed in experiments and can be partly attributed to the $s\bar{s}$ pair production mechanism. It was also predicated that the polarization should also depend on the collision energy $\sqrt{s}$, although early experiments did not find evident signals to confirm this [4, 5, 7]. Recently with an exploration to low energy domain between 7.7 GeV to 27.0 GeV, the RHIC BES I program had successfully observed the energy dependence of Λ polarization with a higher EP resolution and better background extraction.

Using the PICR hydrodynamical model, we calculated the global Λ polarization at the following energies: 11.5 GeV, 14.5 GeV, 19.6 GeV, 27 GeV, 39 GeV, 62.4 GeV, and 200 GeV, and plotted them with red round symbols in Fig. 3. The impact parameter is $b_0 = 0.7$, i.e. the centrality is $c = 49\%$. For comparison the data of Λ and $\bar{\Lambda}$ polarization from STAR (RHIC) were inserted into Fig. 3 with blue triangle symbols. One could see that our model fits fairly well the experimental data. Although the experimental $\bar{\Lambda}$ polarization is larger than the Λ polarization, it will not change the averaged polarization very much, because the production ratio of $\bar{\Lambda}$ to Λ is very small in high energy collisions [35].

Fig. 3 clearly shows that Λ polarization is dependent on collision energy; it drops very fast with increasing energy from 11.4 GeV to 62.4 GeV, and tends to saturate after 62.4 GeV. From thermodynamical perspective, the polarization decreases with energy, and this can be attributed to the higher temperature in higher energy collisions. The drastic thermal motion of particles will decrease the quark polarization rate, which according to Ref. [11] is inversely proportional to the collision energy. One the other hand, simulating results by AMPT has shown that the averaged classical vorticity decreases with the collision energy [36, 37], thus of course leads to the decline of global Λ polarization.

It is also interesting to take a glance on the time evolution of Λ polarization, shown in Fig. 4. In this figure, the Λ polarization increases slowly at early stage, then falls down very fast. The negative polarization values that occur at 62.4 GeV after 10 fm/c, demonstrate the loss of validity of the hydrodynamical model at late stages of system expansion, due to the large surface to volume ratio. Besides, at early stages, no Λs are produced, so the climbing segment of the curves before 4 fm/c is not observable.

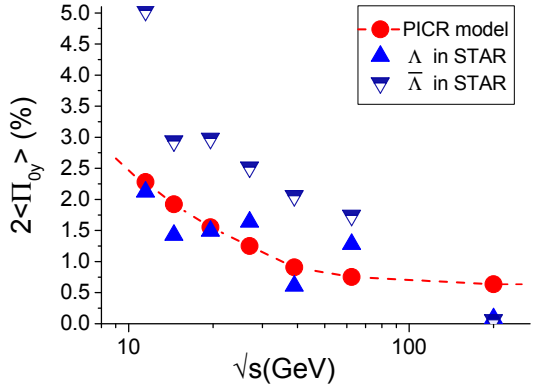

FIG. 3. (Color online) The global polarization, $2\langle\Pi_{0y}\rangle_p$, in our PICR hydro-model (red circle) and STAR BES experiments (green triangle), at energies $\sqrt{s}$ of 11.5 GeV, 14.5 GeV, 19.6 GeV, 27.0 GeV, 39.0 GeV, 62.4 GeV, and 200 GeV. The experimental data were extracted from Ref. [24], with solid triangle for Λ and hollow triangle for $\bar{\Lambda}$, dropping the error bars.

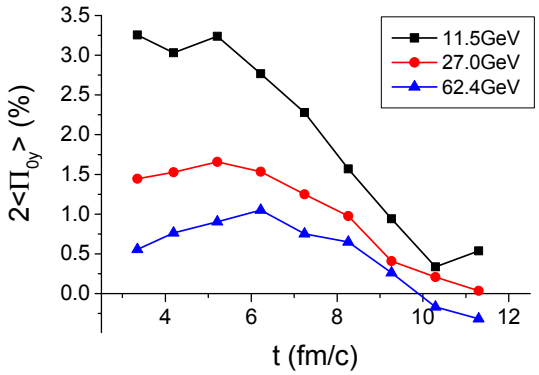

FIG. 4. (Color online) The time evolution of global polarization, $2\langle\Pi_{0y}\rangle_p$, for energy $\sqrt{s}$= 11.5 GeV, 27 GeV and 62.4 GeV.

IV. SUMMARY AND CONCLUSIONS

With a Yang-Mills field initial state and a high resolution (3+1)D Particle-in-Cell Relativistic (PICR) hydrodynamics simulation, we calculate the Λ polarization for different low energies and different impact parameters. The polarization in high energy collisions originates from initial angular momentum, or the inequality of local density between projectile and target, and both of them are sensitive to the impact parameter. Thus, we plotted the global polarization as a function of impact parameter b and a linear dependence on b was observed. We hope that after upgrading the Event Plane Detector, the STAR will provide a higher resolution EP determination and centrality, to determine precisely the centrality dependence of global Λ polarization.

Furthermore, the global Λ polarization in our model decreases very fast in low energy domain, and the decline curve fits very well with the recent results of Beam Energy Scan (BES) program launched by STAR (RHIC).

This is a very exciting new founding which indicates the significance of thermal vorticity and system expansion.

Finally, the time evolution of Λ polarization shows the limitation of hydrodynamical model at later stage of system expansion.

ACKNOWLEDGEMENTS

Enlightening discussions with Mike Lisa, and Francesco Becattini, are gratefully acknowledged. One of the authors, Y.L. Xie, is supported by the China Scholarship Council (China).

[1] G. Bunce, R. Handler, R. March, P. Martin, L. Pondrom, and M. Sheaff, Phys. Rev. Lett. **36**, 1113 (1976).
[2] A. Lesnik, D. M. Schwartzf, I. Ambats, E. Hayes, W. T. Meyer, C. E. W. Ward, T. M. Knasel, 5 E. G. Swallow, and R. Winston II, and T. A. Romanowski, Phys. Rev. Lett. **35**, 770 (1975).
[3] M. Anikina *et al.*, Z. Phys. C: Particles and Fields **25**, 1 (1984).
[4] A. M. Smith *et al.* (R608 Collaboration), Phys. Lett. B **185**, 209, (1987).
[5] E. J. Ramberg *et al.*, Phys. Lett. B **338**, 403-408, (1994).
[6] A. Morelos *et al.* (E761 Collaboration), Phys. Rev. Lett. **71**, 2172, (1993).
[7] I. Abt *et al.* (HERA-B Collaboration), Phys. Lett. B **638**, 415-421, (2006).
[8] I. Selyuzhenkov *et al.*(STAR Collaboration), J. Phys. G: Nucl. Part. Phys. **32**, S557-S561 (2006).
[9] B. I. Abelev *et al.*, Phys. Rev. C **76**, 024915 (2007).
[10] Z.-T. Liang, and X.-N. Wang, Phys. Rev. Lett. **94**, 102301 (2005).
[11] X.-G. Huang, P. Huovinen, and X.-N. Wang, Phys. Rev. C **84**, 054910 (2011).
[12] B. Betz, M. Gyulassy, and G. Torrieri, Phys. Rev. C **76**, 044901 (2007).
[13] F. Becattini, G. Inghirami, V. Rolando, A. Beraudo, L. D. Zanna, A. De Pace, M. Nardi, G. Pagliara, and V. Chandra, Eur. Phys. J. C **75**, 406 (2015).
[14] A. D. Panagiotou, Phys. Rev. C **33**, 1999 (1986).
[15] F. Becattini, V. Chandra, L. Del Zanna, and E. Grossi, Annals of Phys. **338**, 32 (2013).
[16] C.C. Barros and Y. Hama, arXiv:hep-ph/0507013v1.
[17] F. Becattini, L.P. Csernai, and D.J. Wang, Phys. Rev. C **88**, 034905 (2013).
[18] Y.-L. Xie, R.C. Glastad, and L.P. Csernai, Phys. Rev. C **92**, 064901 (2015).
[19] Y.L. Xie, M. Bleicher, H. Stöcker, D.J. Wang, and L.P. Csernai, Phys. Rev. C **94**, 054907 (2016).
[20] L. P. Csernai, G. Eyyubova, and V. K. Magas, Phys. Rev. C **86**, 024912 (2012).
[21] F. Becattini, F. Piccinini, and J. Rizzo, Phys. Rev. C **77**, 024906 (2008).
[22] J.-H. Gao, S.-W. Chen, W.-T. Deng, and Z.-T. Liang, Q. Wang, and X.-N. Wang, Phys. Rev. C **77**, 044902 (2008).
[23] I. Karpenko and F. Becattini, arXiv:1610.04717.
[24] M. A. Lisa *et al.* (STAR Collaboration), Invited talk presented at the QCD Chirality Workshop 2016, Feb. 23-26, 2016, Los Angeles, USA.
[25] T. A. DeGrand, and H. I. Miettinen, Phys. Rev. D **24**, 2419 (1981).
[26] L. P. Csernai, D. D. Strottman, and Cs. Anderlik, Phys. Rev. C **85**, 054901 (2012).
[27] D. Montenegro, L. Tinti, and G. Torrieri, arxive:1701.08263.
[28] L.P. Csernai, D.J. Wang, and T.Csorgo, Phys. Rev. C **90**, 024901 (2014).
[29] V. K. Magas, L. P. Csernai, and D. D. Strottman, Phys. Rev. C **64** 014901 (2001).
[30] V. K. Magas, L. P. Csernai, and D. D. Strottman, Nucl. Phys. A **712** 167 (2002).
[31] L. P. Csernai, Introduction to Relativistic Heavy Ion Collisions, (Jonh Wiley & Sons Ltd., Chichester, 1994).
[32] Y. Cheng, L. P. Csernai, V. K. Magas, B. R. Schlei, and D. D. Strottman, Phys. Rev. C **81**, 064910 (2010).
[33] R.-H. Fang, L.-G. Pang, Q. Wang, and X.-N. Wang, Phys. Rev. C **94**, 024904 (2016).
[34] J.-L. Zhang *et al.* (STAR Collaboration), Invited talk presented at the 16th International Conference on Strangeness in Quark Matter, Jun. 27-July 1, 2016, Berkeley, USA.
[35] T. Anticic *et al.* (NA49 Collaboration), Phys. Lett. B **93**, 022302-1 (2004).
[36] Y. Jiang, Z.-W. Lin, and J.-F. Liao, Phys. Rev. C **94**, 044910 (2016).
[37] W.-T. Deng and X.-G. Huang, Phys. Rev. C **93**, 064907 (2016).